Proceedings World Geothermal Congress 2015
Melbourne, Australia, 19-25 April 2015

New Zealand Geothermal Power Plants as Critical Facilities: an Active Fault Avoidance Study in the Wairakei Geothermal Field, New Zealand

Pilar Villamor[1], Kate Clark[1], Matt Watson[2], Mike Rosenberg[3], Biljana Lukovic[1], Willam Ries[1], Álvaro González[4], Sarah D. Milicich[1], David D. McNamara[1], Bernd Pummer[5], Fabian Sepulveda[5]

[1]GNS Science, Lower Hutt 5040, New Zealand

[2]ScanTec Ltd, Whagarei 0140, New Zealand

[3]GNS Science, Wairakei Research Centre, Taupo 3384, New Zealand

[4]Univesidad de Zaragoza, Zaragoza 50009, Spain

[5]Contact Energy Ltd, Taupo, New Zealand

p.villamor@gns.cri.nz

Keywords: active fault, geothermal power plant, fault avoidance guidelines, ground penetrating radar, paleoseismology

ABSTRACT

Active faults in rifts commonly provide high crustal permeability and control geothermal fluid pathways. However, active faults can also pose surface deformation hazards to geothermal power plants and associated infrastructure. The New Zealand Ministry for the Environment (MfE) guidelines recommend avoidance of active faults for construction of new buildings based on building importance and the rate of fault activity. Power plants, which are classed as 'high Building Importance Category', are permitted on faults with a rupture recurrence interval greater than 10,000 years.

We present a site feasibility study for the Te Mihi Power Plant (Wairakei Geothermal Field), used to determine if there is recent major active faulting at the proposed site. The initial Power Plant site was proposed in an area exhibiting complex surface patterns of active faults with two closely spaced (few metres to hundreds of metres), intersecting, normal fault sets. Detailed aerial photo review and field mapping was undertaken to improve the accuracy of previously mapped fault traces, and to potentially identify previously undocumented faults. Fault scarps were assigned different geomorphic expression (from "clear" to "inferred").

In the study area, recurrence intervals of active faulting can be difficult to estimate because fault scarps are frequently blanketed by tephra from late Quaternary eruptions of the nearby Taupo caldera, and detailed paleoseismic studies are absent. Because of the potential burial of geomorphic fault scarps, GPR surveys and paleoseismic trenching were carried out to investigate the apparent lack of active faulting at the plant footprint, and to better understand fault activity rates close to the newly proposed Power Plant site. Displacements of several post-25 ka tephra marker horizons, and fault planes, were analysed in the trench to assess the presence or absence of recent fault activity, and to calibrate the reflectors observed in the GPR images. The trench study also allowed accurate estimation of fault slip rate and recurrence interval.

This study has provided a first calibration for a correlation between geomorphic expression of faults and fault activity in this area. The study revealed that: a) some of the subtle features initially suspected as fault scarps were indeed active faults; b) deep paleoseismic excavations are needed in sites located in close proximity to frequently active volcanoes (due to thick cover beds) even when assessing faults with clear geomorphic expression; and c) GPR is useful when assessing activity of faults with large offsets (in this area, usually faults with recurrence interval less than 5,000 years), but the resolution of GPR might not allow evaluation of minor faulting which should then be assessed at the site during construction. This investigation allowed the Te Mihi Power Plant to be re-sited in an area outside the identified construction-avoidance envelope that conformed to the recommendations of the MfE guidelines.

1. INTRODUCTION

In the Wairakei Geothermal Field (Fig.1), active deformation along a series of closely spaced, NE-SW trending, high-angle, normal faults provides and maintains fluid pathways in competent rock (greywacke, lava, welded ignimbrite), allowing fluids at shallow levels to move into unconsolidated pyroclastic and sedimentary units (Rosenberg et al., 2009; McLean and McNamara, 2011; Massiot et al., 2013). Whilst these conditions are ideal for geothermal energy development, these active faults can also pose surface deformation hazards to geothermal power plants and associated infrastructure.

The New Zealand Ministry for the Environment (MfE) guidelines for development of land on or close to active faults (Kerr et al., 2003) recommends avoidance of active faults for construction of new buildings and is an important consideration when siting and constructing infrastructure in geothermal fields.. The MfE guidelines adopt a life-safety approach in which buildings are classified based on their importance (power plants are classed as critical facilities, i.e., high Building Importance Category). The hazard posed to infrastructure by fault rupture is quantified using two parameters: a) fault location (extent of deformation), and b) the average recurrence interval of surface rupture (rupture recurrence interval, RI; Table 1). MfE guidelines allow power plant construction on a faults that have a RI >10,000 years. As a consequence appropriate investigations of fault locations and their potential rupture recurrence intervals are essential when determining the suitable location of buildings.

Table 1. Rupture Recurrence Interval (RI) Classes (defined in Kerr et al., 2003).

Recurrence interval class	Average fault recurrence interval of surface rupture
I	≤2,000 years
II	>2,000 years to ≤3,500 years
III	>3,500 years to ≤5,000 years
IV	>5,000 years to ≤10,000 years
V	>10,000 years to ≤20,000 years
VI	>20,000 years to ≤125,000 years

Active faulting studies, including detailed geomorphological mapping of fault scarps and excavation of paleoseismic trenches, in conjunction with Ground Penetrating radar (GPR) surveys have been undertaken both in New Zealand and worldwide to assess active faulting parameters (e.g., Salvi et al., 2003; McClymont et al., 2009, and references therein). Excavation of paleoseismic trenches remains the most accurate approach to assess fault activity because detailed fault parameters such as co-seismic displacement, and timing of individual fault rupturing events (required to estimate recurrence interval and past earthquake magnitudes) are more accurately obtained when the fault plane and displaced geological formations are exposed. However, while less accurate, shallow subsurface geophysical techniques, such as GPR, can add complementary and crucial information such as presence of active faults that do not have surface expression (that is no fault scarp is exposed), and/or total displacement of deeper geological formations that can help in assessing long-term fault slip rates and/or progressive displacement (that is if deeper layers have more displacement than shallower layers, which indicates occurrence of fault rupture in events prior to deposition of the shallower layers). GPR is also a cost-effective and non-invasive technique that is especially useful on large study sites, or if excavations will modify the ground in a way that will affect future use of the land. When used in conjunction, these techniques provide a very powerful method for active faulting characterisation. For example, ages can be assigned to GPR reflectors from trench observations and the preliminary characterisation of a faults activity can be drawn from the GPR images.

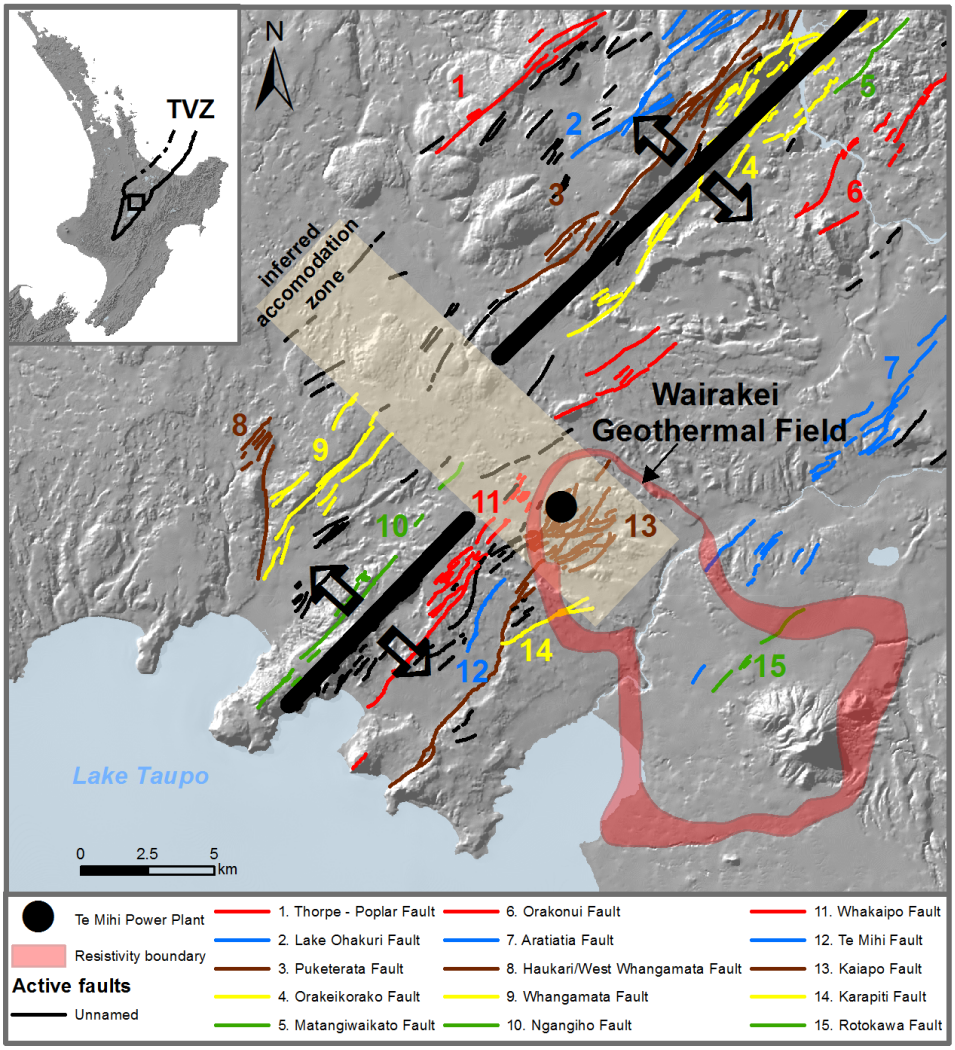

Figure 1. Location of the Wairakei Geothermal Field (resistivity boundary for the Wairakei-Tauhara geothermal system as defined by Risk et al., 1984) and Te Mihi Power Plant within the Taupo Volcanic Zone (TVZ) and local active faults. To the north, the local rift segment is formed by the Orakonui, Orakeikorako, Puketerata, Lake Ohakuri and Tuahu faults that bound a single graben structure. The inferred accommodation zone and rift axes of Rowland and Sibson (2001) are shown.

This paper describes a siting study, conducted between 2005 and 2007 for the Te Mihi Power Plant (Wairakei Geothermal Field; Fig. 1), commissioned in early 2014. The study was designed to determine if there was major (meter-size co-seismic displacements) active faulting at the proposed power plant site. The site was proposed in an area exhibiting complex surface patterns of active faults with two closely spaced (few metres to hundreds of metres), intersecting normal fault sets (fault orientations of N045ºE and N080ºW). Detailed aerial photo interpretation and field mapping were undertaken to improve the accuracy of previously mapped fault traces, and to potentially identify previously undocumented faults, with the aim of determining if the site selection was 'life-safe'. To further explore the presence or absence of active faulting within the Power Plant footprint and to quantify fault activity, GPR and paleoseismic trenching studies were undertaken.

2. GEOLOGICAL SETTING

The Te Mihi area is located within the Wairakei Geothermal Field, Taupo Volcanic Zone (TVZ), a rift system that has been active for the last ca, 1.6 Ma (Wilson et al., 1995). The TVZ is characterised by high crustal heat flow (up to 700 mW/m^2; Bibby et al., 1995), numerous shallow-focus earthquakes (< 8 km deep, at its central latitudes, Bryan et al., 1999), and active extensional faulting (Villamor and Berryman, 2001; Rowland and Sibson, 2001). Tectonic extension in the TVZ is partly accommodated by a dense system of NE-SW trending normal faults that dip both to the NW and SE (Villamor and Berryman, 2001). Rowland and Sibson (2001) described the tectonic structure as a continental rift, here called the Taupo Rift (Acocella et al., 2003), with near-symmetric distributions of opposite-facing normal faults about local axes.

The rift is divided along its length into segments based on structure and volcanology (Rowland and Sibson, 2001; Villamor and Berryman, 2001; Acocella et al., 2003). Within each segment there is a series of well-defined fault sets with predominantly NE-SW strike orientations which taper out at the end of the segment. The switch from dominantly SE dipping to NW dipping faults in each of these segments has been used to infer the location of a 'rift axis' in each segment(Fig. 1: Rowland and Sibson, 2004). The offsets between segment axes are used to infer the presence of accommodation zones where the tectonic deformation of one segment is transferred to the other (Fig. 1). In various areas of the Taupo Rift, these accommodation zones are described as hard-linked (transfer/strike-slip faults) and soft-linked (relay structures) (Rowland and Sibson, 2001; Spinks et al., 2005; Seebeck et al., 2010; McNamara at al., 2013). Soft-linked accommodation zones can present a series of stepped-over, short, normal faults that are disconnected at the surface. In contrast to this, a hard-linked accommodation zone can be represented by strike-slip faults, often perpendicular to the rift axis. It has been proposed that the accommodation zones of the Taupo Rift are soft-linked in the upper sections of the crust (at least <3 km) and that in deeper levels they are expressed as hard-linked (Rowland and Sibson, 2004).

The Te Mihi area is potentially located within one of these inferred accommodation zones (Fig. 1). South of this area the rift is clearly defined by a series of horsts (uplifted blocks between two normal faults that dip outwards from the block) and grabens (subsided blocks between two normal faults that dip towards the block) that are bound by the major faults known as the Aratiatia, Kaiapo, Whakapio, Ngangiho, and Whangamata faults (Litchfield et al., 2014). To the north, the local rift segment is formed by the Orakonui, Orakeikorako, Puketerata, Lake Ohakuri and Tuahu faults that bound a single graben structure (Litchfield et al., 2014).

The deposits that cover the landscape at Te Mihi are mainly volcanic ash or ignimbrites erupted from Lake Taupo (see Wilson, 1993, for full description of late Quaternary eruptions from Lake Taupo). Key units in the study area have been dated in other studies using radiocarbon techniques and are listed in Table 2. The ages of the volcanic deposits are used in paleoseismic studies to constrain the timing of individual earthquake events.

Table 2. Age of volcanic units identified in this study

Unit	Age (calibrated years B.P.*)	References
Taupo Formation (including Taupo Ignimbrite and Rotongaio Tephra)	1718 ± 30	Sparks et al. (1995)
Whakaipo Tephra	2762 ± 20	Gehrels et al. 2006
Waimihia Tephra	3410 ± 40	Hajdas et al. (2006)
Opepe Tephra	10,075 ± 155	Hajdas et al. (2006)
Karapiti Tephra	11,410 ± 190	Hajdas et al. (2006)
Oruanui Ignimbrite	25,360 ± 160	Vandergoes et al. (2013)

* B.P. = before present (1950)

Prior to this study, the faults in the Te Mihi area had been mapped by Grindley (1965), Ted Lloyd (fieldwork for unpubl. 1:50k geology map) and Debbie Fellows (1989; GNS active fault database at initiation of project, 2005). While the two former studies mapped all possible fault lines, using surface and sub-surface studies (geomorphic expression of fault lines, surface geology and subsurface data from drill holes), Fellows' compilation concentrated exclusively on active traces (faults with clear geomorphological expression and fault plane outcrops).

In the Te Mihi area, the age of the fault scarps (Fig. 2) can be approximated to the age of the main geomorphological features that are offset by active faults. These are:

a) the **constructional surface** of the 25,400 year old Oruanui Ignimbrite (Fig. 2). The ignimbrite was erupted from Lake Taupo and covered the landscape around the lake, filling all the valleys and forming an extensive plateau (Manville and Wilson, 2004). Remnants of that surface today correspond to the highest plateaus and ridges in the Te Mihi area.

b) the **slopes** created by river incision into the Oruanui Ignimbrite constructional surface. Shortly after the end of the 25,400 year old Oruanui eruption, surface water eroded into the soft ignimbrite forming the current drainage system (Manville and Wilson, 2004).

c) the **valley floors or terraces** of the stream and rivers that were incised into the ignimbrite constructional surface. There are two types of valley floors: i) valley floors that where abandoned by the drainage system when the climate changed from cold conditions to moderate conditions (see example in Fig. 2) and ii) the current valley floors. The former have higher altitudes and represent an older surface (possibly c. 15,000-18,000 years when compared to similar valleys in the Rotorua area; Villamor and Berryman, 2001). The latter are the current active valley floors that became the main drainage system when rapid incision followed the increase in rainfall during the warming period. The current valleys were partially filled by the 1,700 year old Taupo Ignimbrite which did not reach the height of the Oruanui constructional surface.

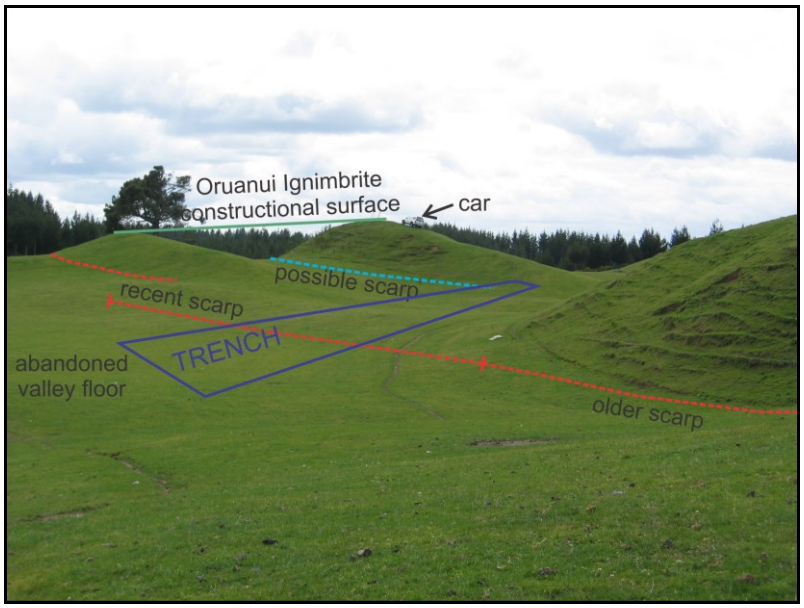

Figure 2. Varied geomorphic expression of fault scarps in the Te Mihi area. Note car parked on the top of the central ridge for scale.

3. METHODS

3.1. Fault mapping

Mapping of faults in the Te Mihi area was carried out by: a) identifying as many active fault traces as possible, and b) mapping and defining the coordinates of the fault traces. The identification of traces was mainly achieved by aerial photo interpretation, followed by field reconnaissance to identify fault scarps. After identification of fault scarps, we mapped them onto a one-metre-resolution orthophotograph and a one-metre-contour topographic map. The accuracy with which the location of a fault feature can be recorded on a map is influenced by two uncertainties:

1. **Feature error**: how accurately the feature can be located on the ground, i.e., whether the fault has good geomorphic expression. The highest resolution is obtained when the actual fault plane is exposed (natural outcrop or exploratory trench) and identified. Reasonable resolution can be obtained when a clear fault scarp is identified on aerial photos and/or the ground. However, a geomorphic fault scarp has a certain width from the bottom to the top and the fault plane itself can be located anywhere across the width of this step; thus the location is somewhat less certain than if the fault plane is exposed. Poor resolution occurs when the fault scarp cannot be located on the ground surface (i.e. it has been eroded away, covered by vegetation, and/or buried by young sediments). For this purpose we classified the fault traces, in order of decreasing accuracy in fault location, into:

    a) "*fault scarp*" - a linear geomorphic feature or step in the ground clearly identified as having a tectonic origin, and represented by a sharp step in the ground with a narrow scarp width that can be easily mapped.

    b) "*possible fault scarp*" - a linear geomorphologicalc feature or step in the ground that resembles a fault scarp but has a potentially different origin (e.g. fluvial) and is often represented by a subtle step with a larger scarp width.

    c) "*inferred trace*" - where geological and geomorphological observations suggest a non-visible fault trace may be present, e.g. a fault scarp may extend across a valley but fluvial processes have eroded a section of the fault.

2. **Capture error**: error associated with transferring that position onto a map. This is ultimately dependent on the quality and scale of the base map. In this study when a fault feature was identified on the ground or from aerial photos, whether the feature was distinct or otherwise, and its position was captured/defined using orthophotography, we assigned the highest capturing resolution. More often, we captured the feature on the rectified aerial photos. High accuracy rectification of aerial photos is not always possible because distinct features common to both the original aerial photo and the more recent orthophoto may not be present, and thus the potential for error is larger if older rectified photos are used as the base map instead of the recent orthophoto.

The criteria for assigning uncertainty in fault location from these two factors are shown in Table 3. To achieve a more accurate location of the mapped fault traces, detailed site specific exploration techniques and topographic surveying are required.

Table 3. Fault location uncertainty

Fault features	Capture map	Location Uncertainty (combined feature- and capture error)
Scarp	Orthophoto	± 10 m
Scarp	Rectified aerial photo	± 15 m
Possible scarp	Orthophoto	± 25 m
Possible scarp	Rectified aerial photo	± 25 m
Inferred trace	-N/A-	± 50 to 100 m*

* The uncertainty in location for inferred traces depends on how close the surrounding faults are, and thus increases with the length of the inferred trace itself.

3.2. Correlation between fault activity rate and fault scarp geomorphic expression

Aerial photo interpretation and field mapping are not exhaustive, as active fault traces may have been eroded or buried and therefore not identifiable during initial mapping. To further explore the presence or absence of active faulting and gain insight into the fault activity rate of any mapped fault features, paleoseismic trenching studies and GPR surveys have been undertaken. These surveys aimed to assess the exact location of fault planes by identifying offset layers (reflectors) from GPR images, and the Recurrence Interval Class (RI) of the faults by exposing selected faults through trenching and analysing the age of displaced tephra layers. Using the geomorphological and geometric relationship between dated tephra and other units (Table 2), it can be determined from GPR lines and within fault trenches and road-cut exposures whether layers of different ages have been offset by faulting. Where GPR results confirm the presence of faulting within proposed geothermal power plant sites, the plant footprint should be relocated to avoid that feature. The location of the paleoseismic trench and GPR lines undertaken at Te Mihi for this study are shown in Fig. 3.

GPR data were collected using a GSSI SIR-10A+ radar system with 500MHz and 200MHz frequency antennae. Measurements were recorded from a 4WD vehicle, while driving along pre-marked survey lines at approximately 2 to 3 km/hr. An acquisition rate of 100 scans per second was used with GPR data synchronised with GPS data recorded using a 10 Hz Trimble Omnistar real-time correction differential system. Positional accuracy is <0.5 m horizontally and vertically. All data files were processed using RADAN 6.5 software. This involved frequency filtering (FIR high pass, FIR low pass), background removal, predictive deconvolution, linear gain adjustments and Kirchoff migration. Topographic corrections were applied to all GPR data.

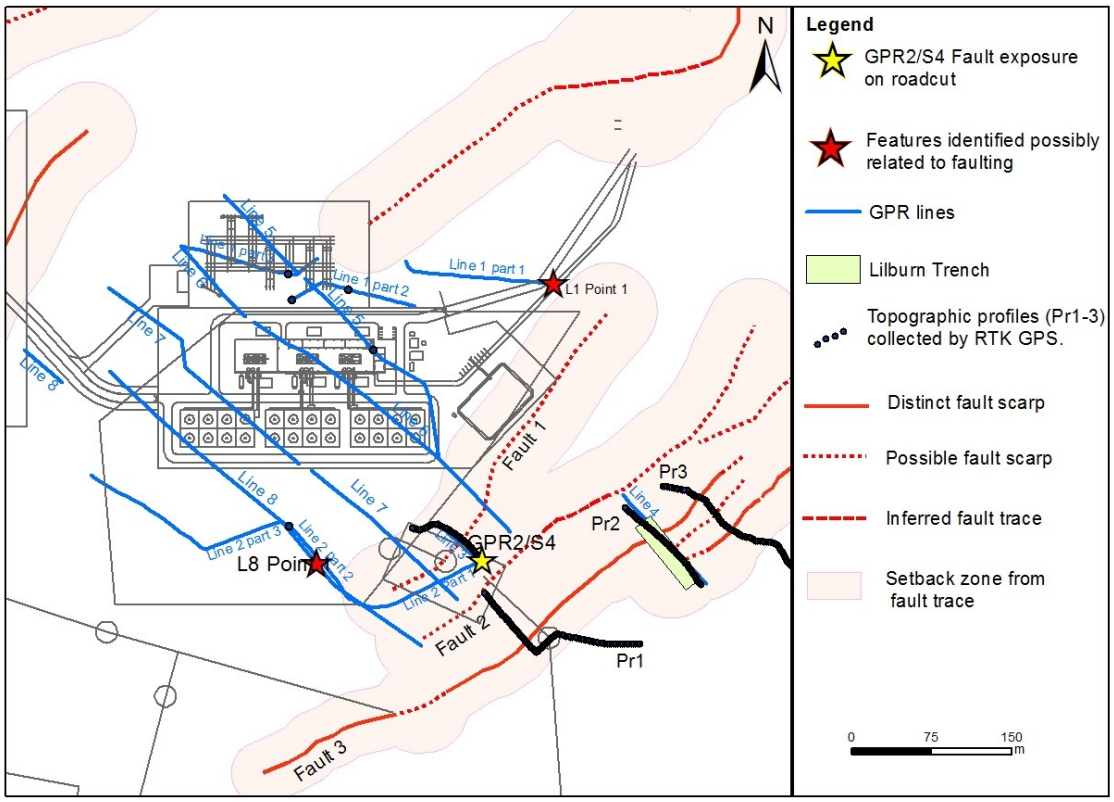

Figure 3. Location of GPR lines, paleoseismic trench and logged outcrop around the proposed site of the Te Mihi Power Plant infrastructure. The classification of fault scarps is as per initial mapping prior to excavation of trenches and GPR survey.

During this investigation, we excavated one trench, named Lilburn Trench (Fig. 3), across an active fault scarp with a geomorphological expression that indicated the highest potential rate of activity close to the proposed Te Mihi Power Plant. The trench was 62 m long and ~6.5 m deep. In cross-section the trench wall that was studied (NE wall) was excavated in 1.5 m high vertical batters and 1 to 1.5 m wide benches with a ~ 4 m wide floor at the bottom of the trench. The opposite wall was excavated with a <35º slope in accordance health and safety best practice. The NE wall of the trench was smoothed, cleaned and the geological features were logged at 1:20 scale on gridded paper. This was accompanied by detailed descriptions of geological materials, measurements of the orientations of geological structures, and notes on the relative history of deformation. *In-situ* volcanic tephra identification was undertaken through correlation with known type sections to assign ages to the different layers. Key locations on the trench were also surveyed using Real-Time Kinematic (RTK) GPS (Fig. 3) so as to match them to the GPR line and locate the active fault coordinates precisely. The study also undertook RTK-GPS surveys of ground surface profiles for considerable distances upslope and downslope of the trench to quantify the extent of ground deformation associated with the active fault. A new road-cut exposure was also examined on a farm (location GPR2/S4 in Fig. 3) and showed a fault plane associated with a mapped possible fault scarp. The area of the fault plane was also cleaned and photographed, and notes were taken on the recent displacement history of the fault.

Displacements of several post-25 ka tephra marker horizons, and fault planes, were analysed in the trench to assess the presence or absence of recent fault activity, and to calibrate the reflectors observed in the GPR images. The trench study also allowed accurate estimation of fault slip rate and recurrence interval. GPR images across the trench helped to assess the amount of displacement of the Oruanui Ignimbrite (~25,400 yr) at each fault plane.

4. RESULTS

4.1. Avoidance zones and siting of the plant

Figure 4 provides a representative example in the study area which graphically depicts the location accuracy of each fault trace using a zone with an appropriate uncertainty width (instead of a simple line) to plot the fault traces (this band represents the location uncertainty of Table 3). A 20 m buffer has also been added to either side of the mapped zone to account for the area of deformation expected to be associated with fault rupture, as recommended in the MfE Guidelines (Kerr et al., 2003). This buffer around each active fault, comprising both location uncertainty and 20 m setback, represents the Fault Avoidance Zone. Mapping of active faults in the Te Mihi area achieves a minimum location accuracy of ± 10 m (where the fault feature is sharp and distinct) and could reach up to ± 100 m (where the fault cannot be identified easily).

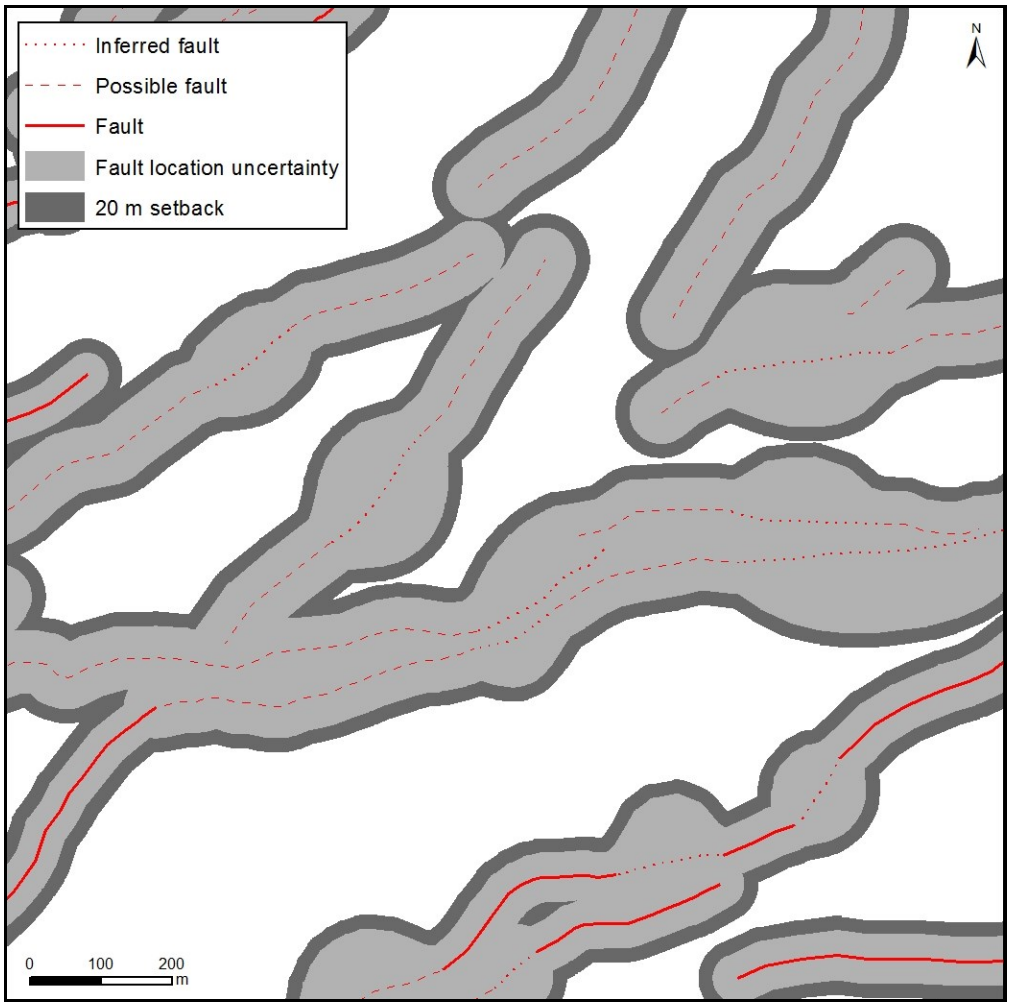

Figure 4. A representative example of location accuracy for mapped fault traces.

Based on the new fault mapping in the Te Mihi area, a number of previously unknown active faults were identified (most of them with subtle geomorphological expression). Some of the newly mapped faults which have an ENE trend, were already observed by Grindley (1965), although were not commonly mapped in the area. Figure 5 shows a comparison between the previous active fault map and the results of this study. Taking into account the new faults, the proposed site for the Power Plant was relocated to a new site (Fig. 5).

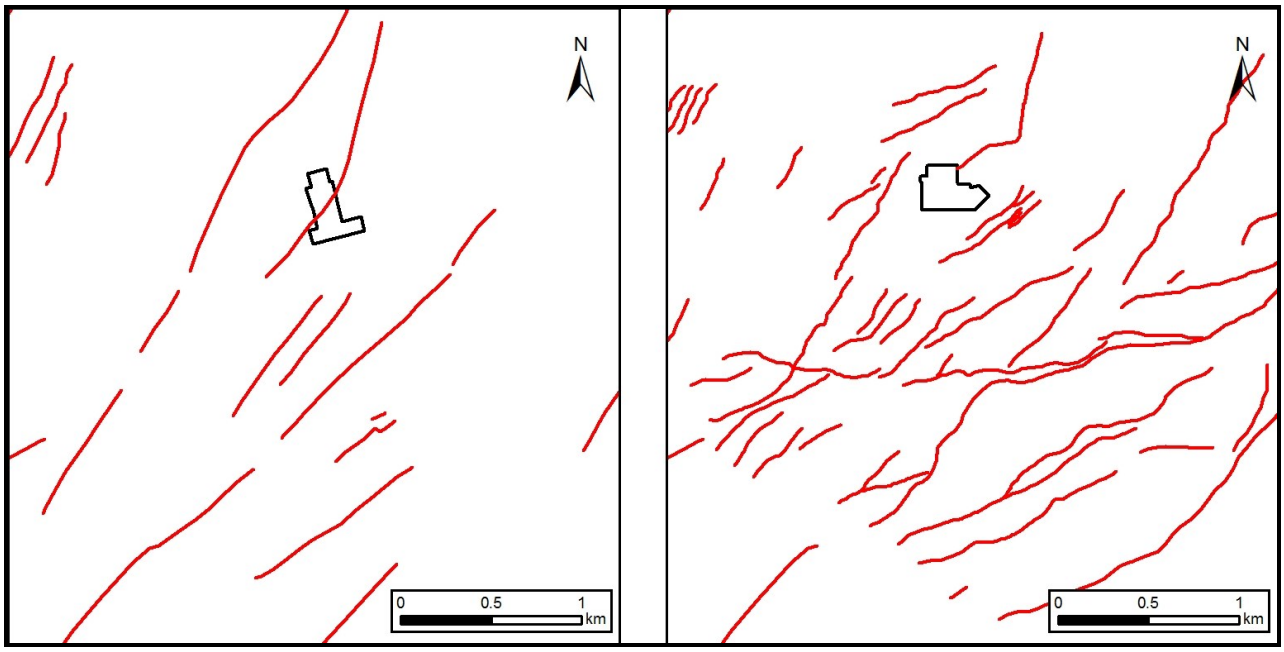

Figure 5. The impact of fault mapping on the final location of the Te Mihi Power Plant. Left: location of known active faults prior to this study and initial proposed site of the Te Mihi Power Plant. Right: location of active faults mapped in this study and the subsequent location of the Te Mihi Power Plant.

4.2. Site specific exploration and topographic surveying

Further exploration of the new proposed site was undertaken with GPR and paleoseismic trenching (Fig. 3). GPR line 4 was run along the Lilburn trench (Fig. 3), and both are directly compared in Figure 6 as an example of this work.

Three strands of the Kaiapo Fault (Figs. 1&3) pass close to the proposed Power Plant site (Fig. 3) and were investigated with GPR and paleoseismic trenching. Here we describe results for each of the faults.

Fault 1: Fault 1 consists of a single fault scarp and is potentially the active fault closest to the new Power Plant site. Its geomorphological expression is very subtle with a broad scarp on the remnants of the Oruanui constructional surface but no scarp across the Holocene valley floors. As such, it was originally mapped as a possible fault scarp. GPR lines 2 and 3, which cross the Fault 1 scarp, show no expression of faulting. However, during excavation of the Power Plant site, evidence was found of active faulting in this location, illustrating how difficult it is to locate with small offsets using GPR.

Fault 2: Fault 2 consists of a single fault scarp close to the Power Plant but splays into two fault scarps to the north. Recent cuttings associated with the construction of a pipe line have exposed two fault planes which correspond to Fault 2 in the area where the geomorphological expression of the fault appears to be a single fault scarp. The presence of faulting confirmed that Fault 2 scarp represents an "active fault" rather than a "possible active fault". The road-cut exposure at location GPR2/S4 (Fig. 3) is almost parallel to the fault planes, which makes them difficult to observe. Nonetheless the exposure shows two normal fault planes (fault planes 1 and 2, Fig. 7) with a NE-SW strike and dipping steeply to the SE. The total offset of the lowermost identified unit, the Karapiti Tephra, corrected due to viewing angle, is ~ 60 cm. This is similar to the total height of the geomorphological scarp (~1 m), which represents the total offset of the top of Oruanui Ignimbrite constructional surface. This total offset is very small, suggesting that the Fault 2 scarp is possibly a secondary, antithetic (i.e., with a fault dip opposite to that of the main fault) fault to the main Fault 3. The progressive displacement of older units in relation to the younger units in the Fault 2 exposure provides good evidence for two or three earthquakes (Table 4, Fig. 7).

Fault 3: Fault 3 clearly displaces the post Oruanui geomorphological surface by 10.5 m. Fault 3 consists of three fault scarps on the Oruanui geomorphiological surface, a 'distinct fault' scarp to the SW and NE, and 'possible fault' scarp between these two. These three scarps are positioned structurally so that they form a right step-over (Fig. 3). The 'distinct fault' scarps to the SW and NE also displaces the valley floor (Holocene surface) to form two subtle ~1 m high scarps.

The Lilburn trench was excavated across the three fault scarps of Fault 3. Exposed on the westernmost part of the NE wall of the Lilburn trench was a thick sequence (up to 6 m) of Taupo eruption deposits, which, because of their thickness, precluded the complete exposure of faulting in the underlying sequence of older materials. Towards the middle and easternmost sections of the trench wall, a complete sequence of post-Oruanui Ignimbrite tephras and the top of the Oruanui Ignimbrite were exposed in the footwall blocks of the fault strands. GPR line 4, parallel with the trench, identified reflectors associated with the top of the Oruanui Ignimbrite that showed a topographic high at the location of the mapped fault scarps which represent ~4 m of accumulated displacement (Fig. 6).

Paleoseismic analysis identified and bracketed the age of faulting events (earthquakes). Faulting in the Lilburn trench comprises of three fault zones A-C (Fig. 6). At fault zone A, one clear faulting event and a further three possible events can be identified (Table 4), including a post-Taupo eruption fault rupture (Event F3_1; post ~1,718 cal. yr. B.P.). At fault zone B, the fault plane is barely exposed but the geometric relationships among different volcanic units suggests there is a fault with a SE down-throw observed (antithetic to the major fault zones A and C). An erosional unconformity below the Waimihia Tephra (Unit 7d; ~ 3,410 cal. yr. B.P.) suggests faulting prior to deposition of this unit. There does not seem to be any faulting post-Waimihia Tephra (Unit 7d), explaining why deposits younger than Waimihia are not eroded and how they mantle the pre-existing geomorphological scarp. Thus no clear displacement of the valley floor is observed at this location. At fault zone C, the upper ends of several normal fault planes are exposed (Fig. 6). These fault planes have a strike trend of N085-095ºE, oblique to the trench wall (N135ºE) complicating their observation and interpretation. The fault planes are steeply dipping to the NW. At this location there is no evidence of displacement in the Taupo deposits (units 3d, and 2e), and as a consequence no evidence for Event F3_1 and Event F3_2 (Table 4). Event F3_3 is represented by the displacement of older units up to the Whakaipo Tephra (Unit 5c; ~ 2,762 cal. yr. B.P.) along the fault plane. This fault plane is covered by non-displaced Rotongaio Tephra (Unit 3d; belongs to the Taupo eruption). Prior to Event F3_3 deformation of older units including the Opepe Tephra (Unit 9; ~10,075 cal. yr. B.P.) is expressed in a few fault planes that do not extend upwards into the Waimihia Tephra (Unit 7d). This deformation is associated with Event F3_4 (Table 4).

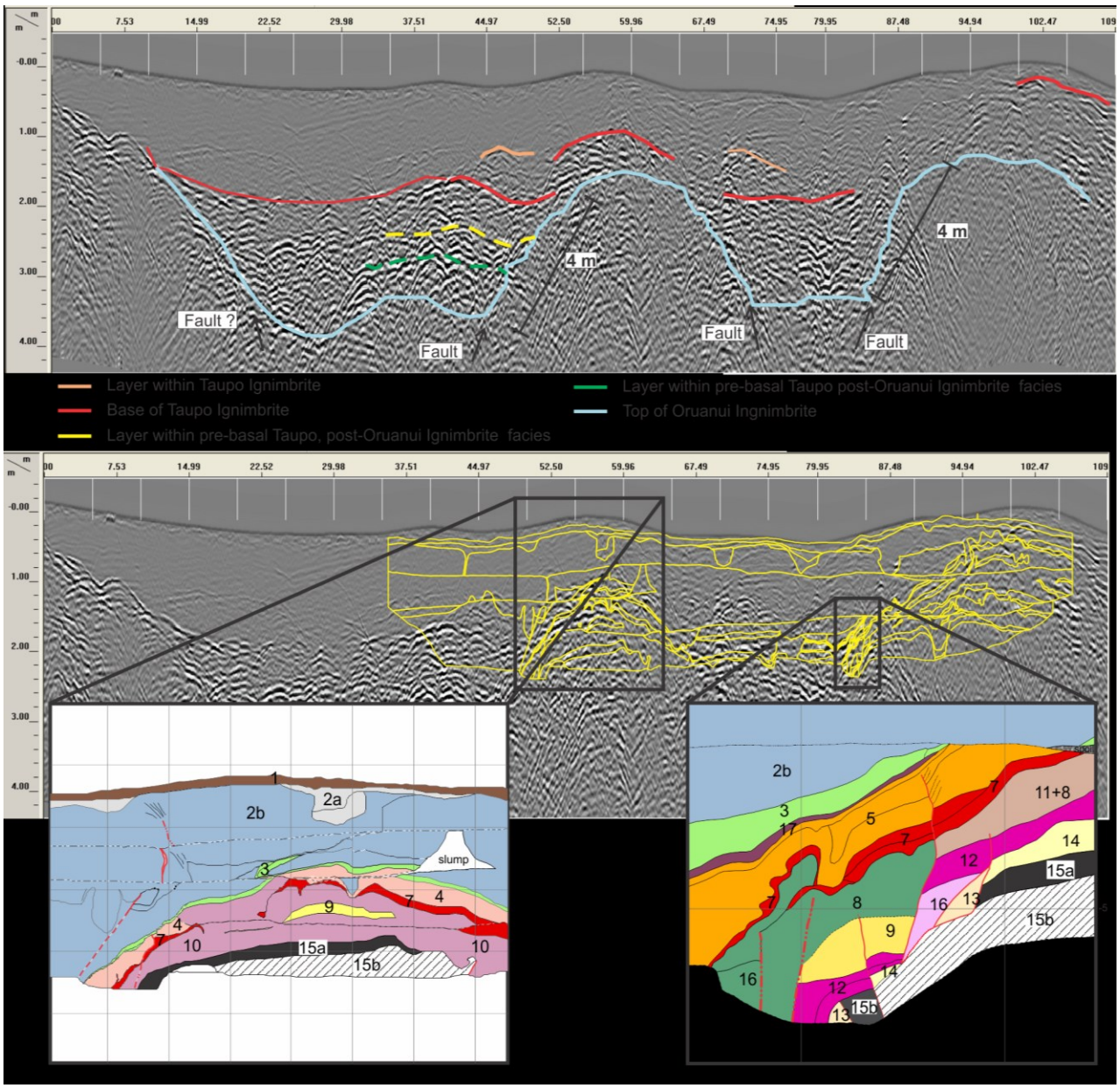

Figure 6. Direct comparison of GPR line 4 and sections of the Lilburn trench. The upper GPR image shows distinguishable reflectors correlated in the trench with known tephra or ignimbrite, while the lower GPR image shows the detailed Lilburn trench log transposed directly onto the GPR radiogram. The expanded view inset panels are examples of the detailed logging from the trench face. Tephra and paleosol units are: 1, Topsoil; 2a, Taupo pumice alluvium; 2b, Taupo ignimbrite; 3, Rotongaio; 4, Post-Waimihia to pre-Rotongaio units; 5, Whakaipo; 7, Waimihia; 8, Post-Opepe to pre-Waimihia units; 9, Opepe; 10, Mixed post-Oruanui to pre-Waimihia units; 11, post-Karapiti to pre-Waimihia units; 12, Karapiti; 13, loess; 14, Post-Oruanui to pre-Karapiti; 15a, Oruanui ignimbrite reworked; 15b, Oruanui ignimbrite reworked 16, Mixed tephra-paleosol package; 17, Hatepe.

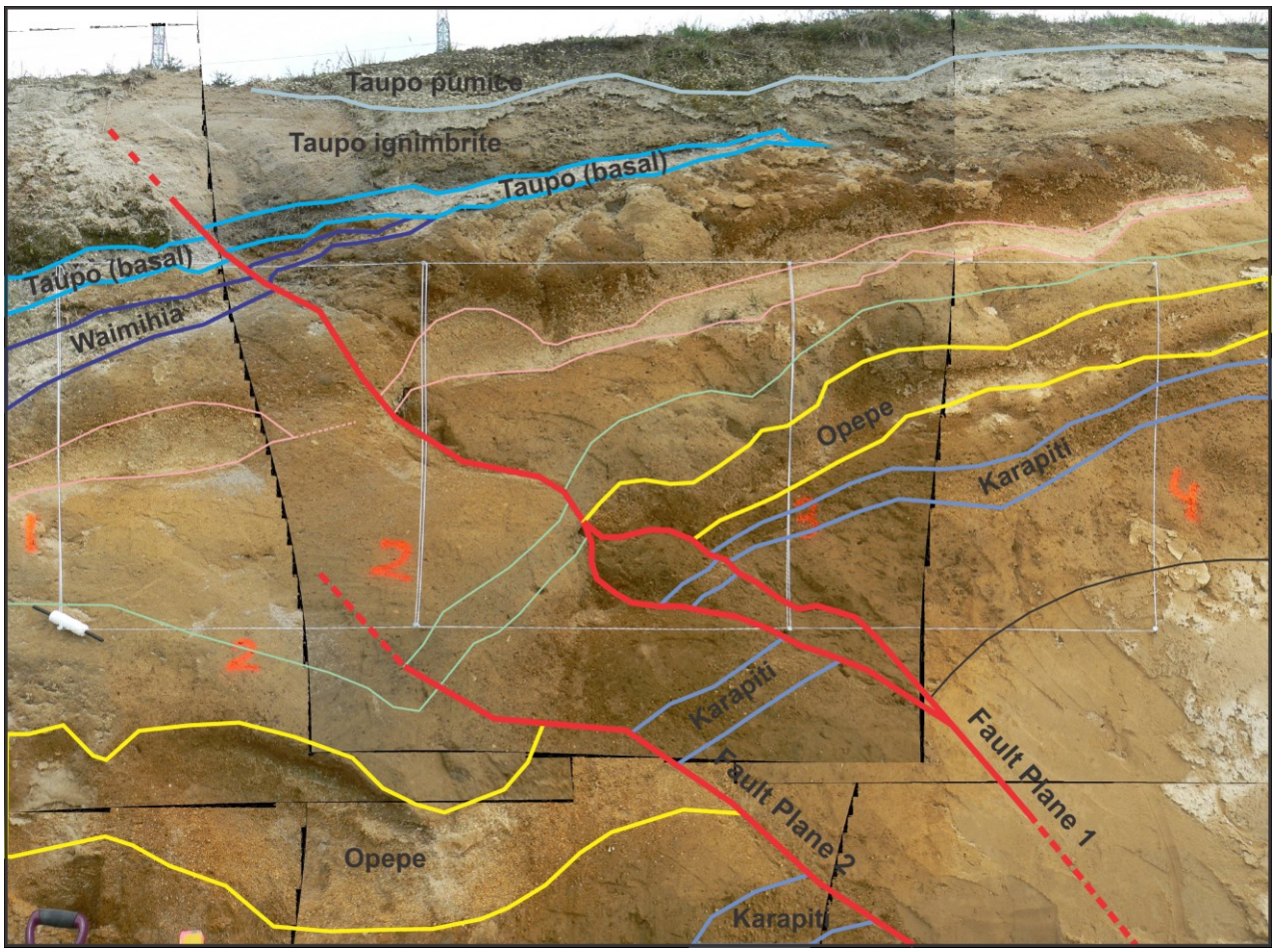

Figure 7. Detailed logging of the road-cut exposure at location GPR2/S4 (Fig. 3) is presented as an example of paleoseismic logging. This site is across the expression of Fault 2, represented at this site by two fault planes (note that apparent dip to NW is an artifact of the sub-parallel orientation of the fault plane with respect to the wall and the irregular surface of the road-cut).

Table 4. Faulting events at Faults 2 and 3 (strands of the Kaiapo Fault) and fault Recurrence Interval Class.

	Events at Fault 2	**Events at Fault 3, zone A.**	**Events at Fault 3, zone B.**	**Events at Fault 3, zone C.**	**Events both faults (F2 + F3)[#]**
Post - Taupo (post 1,718 yr. B.P.)		Event F3_1			Event 1
Intra -Taupo eruption (1,718 yr. B.P.)	Event F2_1*	Event F3_2*			Event 2*
Post - Waimihia/Whakaipo, Pre - Taupo (post 3,410/2,760 – pre 1,718 yr. B.P.)		Event F3_3	Event F3_3	Event F3_3	Event 3
Post Opepe - pre Waimihia (post 10,075 – pre 3,410 yr. B.P.)	Event F2_2	Event F3_4		Event F3_4	Event 4
Post Karapiti - pre Opepe (post 11,450 – pre 10,075 yr. B.P.)	Event F2_3				
RECURRENCE INTERVAL CLASS (years)	IV (~5,725)	II to III (3,360 to ~5,000)	V to VI (>10,075)	III (~5,000)	II to III (3,360 to ~5,000)

*Event 2 is related to volcanism and it is not included in the calculation of the Recurrence Interval Class.
[#]Faults 2 and 3 are likely to be part of the same major fault.

5. DISCUSSION

5.1 Fault recurrence intervals in the Te Mihi area

Three major fault scarps belonging to the Kaiapo Fault were mapped close to the proposed Te Mihi Power Plant site (Fig. 3) and, as a consequence the Power Plant was sited outside the avoidance zone of these faults. The two westernmost fault strands were originally mapped prior to trench excavation and GPR survey as "possible fault scarps" (Fault 1 and 2) and the eastern fault was described as a "clear active fault" (Fault 3, Fig. 3). Evidence indicates that these three faults most likely belong to the same major fault strand and that they merge into a single fault at depth. Therefore, they can be considered as the same fault zone.

Unfortunately, because in most cases the top of Oruanui Ignimbrite and older deposits on the down-thrown side of the faults were not exposed, the occurrence of faulting events for the period between the time of Opepe and Oruanui deposition (10,075 – 26,000 yr. B.P.) cannot be resolved. This adds uncertainty to the RI class estimates. While all fault strands have not always ruptured together, they can still be considered a single fault plane at depth. It is common that faults that branch upwards into numerous fault strands do not always display surface rupture in all fault strands during a single event (e.g. Berryman et al., 2008). However, as suggested by the recent geomorphological expression, zone A in Fault 3 seems to be a principal fault strand and better represents the recurrence interval for the subsurface rupture of the fault.

Results from the Lilburn trench provide a first correlation between geomorphological expression and RI class. In general antithetic fault zones, represented by Fault 2 and Fault 3 (zone B), have a RI Class of IV to VI, while major synthetic fault zones, represented by Fault 3 (zones A and C), have a lower RI Class (II to III). As a general and preliminary approach to characterising recurrence classes for faults in this area, it seems that subtle or possible fault scarps (if confirmed to be active faults) probably belong to Recurrence Interval Class IV to VI, while distinct or clear scarps are more likely to belong to Recurrence Interval Class II to III.

Fault 2 exposed in the road-cutting gives additional information to aid the interpretation of possible fault scarps. Fault 2 showed ~60 cm offset of the Karapiti tephra (oldest tephra exposed; 11,450 yr. B.P.), and ~ 1 m offset across the Oruanui Ignimbrite surface. The GPR line at this location displayed no clear displacement of the older Oruanui Tephra (25,400 years), which should have an equal or greater displacement to that of the Karapiti tephra. This confirms that displacements of the Oruanui Ignimbrite of <60 cm (possibly even < 1 m) will not be detected by GPR. However, these faults are likely to have recurrence interval belonging to RI Class IV+, or if RI is shorter they will only have small displacement per event (e.g., average per event displacement for Fault 2 of ~20 cm).

The information gathered from the GPR across the trench and road-cut site were assisted with the interpretation of the presence or absence of faulting in the proposed Power Plant footprint. Some of the steps in the reflectors have been interpreted as being related to erosion based on analysis of the type of geometric relations between different GPR reflectors, or due to the lack of lateral extension of the step into nearby GPR lines. Only two of the Oruanui topographic highs (steps in reflectors), L1_point 1 and L8_point1 (Fig. 3), are potential fault planes, but they are located tens of metres away from the Power Plant site and they do not extend to within 20 m of the site (as shown by their absence in other GPR lines). Accordingly, even if they are active faults, they do not pass through the site, and do not represent a rupture hazard to the site.

The resolution of the GPR study does not allow the evaluation of minor faulting, i.e., faults with accumulated displacements of < 0.6 – 1 m since ~ 11,450 to 26,000 yrs B.P. Such minor displacements would also be difficult to delineate as fault scarps during aerial photo review. Minor fault traces are expected to represent low hazard. Small accumulated displacements could be either a consequence of very small displacements (< 0.25 m) that occurred often (e.g., recurrence interval 3,500 to 10,000 years, or RI Class of II to IV) or of somewhat larger displacements (~ 0.25 – 0.5 m) that occur seldom (i.e., recurrence interval > 10,000 years, or RI Classes of V or VI). It is suggested that small features such as this could be analysed in greater detail during the excavation of construction sites, with the results used to fine tune the location and/or building design.

5.2. Implications for siting critical facilities in areas proximal to large ignimbrite producing volcanic centres

Eruptions from large silicic volcanic centers tend to fill the proximal landscape with volcanic deposits (e.g., Manville and Wilson, 2004) that affect the analysis of active fault rates in several ways. Airfall deposits mantling the fault scarps typically provide chronological markers that are essential to assess the relative timing of fault rupture and thus fault recurrence intervals. Except for extremely proximal areas, airfall deposits may not bury a scarp entirely, so the fault can be mapped by aerial photogrammetry, topographic analysis and field reconnaissance. However, airfall deposition frequently subdues geomorphological expression through deposition of thicker sequences on the down-thrown side of the scarp. This causes the feature to be less recognisable as a fault scarp. Ignimbrite sheets, although good chronological markers, tend to obscure faulting because they fill valleys and greatly modify the landscape. Valley-ponding ignimbrite deposits could bury a fault scarp so that the fault is either not identifiable, or if identified where it displaces higher and older surfaces, the lack of displacement of the Holocene valley surface may cause the fault to interpreted as either extinct or not very active. In addition, tephra-derived alluvial deposits can fill valleys, often at great distances from the eruption vent and in events occurring decades to centuries after the associated eruption, thereby obscuring fault activity (Manville and Wilson, 2004).

In the area around the Taupo Volcanic Centre, the Oruanui eruption created a major constructional surface (Manville and Wilson, 2004) that has been essential in identifying and mapping recent faults. However, tephra from post-Oruanui eruptions and, more importantly, infill of Holocene valleys by the ~1.8 ka Taupo Ignimbrite, have obscured a large part of the active fault network, so that only the fastest slipping fault strands are easy to identify. The recent mapping presented in this study differs considerably from earlier maps, as it considers and proves that some of the subtle “possible faults” are indeed active faults.

The results of this study are important when siting critical facilities, in particular geothermal power plants and infrastructure, which, due to the nature of the geothermal resource, tend to be close to active faults in volcanic environments. Our results suggest that detailed analysis of the subtle landforms within an active fault network in areas of profuse volcanic deposition or sedimentation is essential to assess seismic and surface rupture hazards to critical facilities. Those subtle features need to be further analysed with other methods that can either expose or image the faults to establish a correlation between the type of geomorphic expression of the fault scarp and the actual fault activity rate. Our study in the area proximal to the Taupo Volcanic Centre has established a preliminary correlation between scarp geomorphic expression and fault activity rate. While our study has sound results, we believe there is a need to refine this correlation with further investigation. In particular it is important to assess how the correlation between fault activity rate and active fault geomorphic expression varies spatially for increasing distances to the eruption source.

6. CONCLUSIONS

For construction of critical facilities, such as geothermal power plants, the New Zealand Ministry for the Environment (MfE) Guidelines suggests avoidance of faults with an activity recurrence interval ≤ 10,000 years (i.e. Recurrence Interval Class ≤ IV from MfE guidelines). Aerial photography of active fault scarps, GPR transects and detailed trench logging were successfully applied in a fault avoidance study of a proposed site for the Te Mihi Power Plant, Wairakei Geothermal Field, New Zealand.

The Te Mihi study shows that a focused multi-disciplinary approach is essential to inspect, define, and categorise faults according to magnitude and frequency of their rupture, particularly where their geomorphic expression is subtle or obscured. It is clear that substantial differences in fault location and delineation from those marked by broad scale mapping can be highlighted by detailed study and are critical to establish for application of fault avoidance guidelines.

Defining known and additional fault locations and establishing rupture recurrence classes gave rise to substantial modification of the site footprint, such that there are now no active faults within the footprint and all buildings and infrastructure are now more than 20 m from active faults. By major active faulting for this area, we refer to faults that are clearly visible on aerial photographs or GPR images and that typically have a recurrence interval class between I and VI (i.e. ≤ 10,000 years). We cannot rule out the presence of minor faulting (displacement <0.5 m since 10,000 – 26,000 yrs B.P.) because these could not be resolved with the available techniques. However, minor faults (with co-seismic displacements of 0.25 – 0.5 m) are likely to have Recurrence Interval Class of V or VI (i.e. ≥ 10,000 years). Minor faults could, alternatively, have smaller recurrence intervals (3,500 – 10,000 years) but also much smaller displacements (<0.25 m). In either scenario, they present a low seismic hazard.

The principles and methods used for the mapping and characterisation of fault activity in this area are applicable to other areas worldwide, particularly those located in volcanically and tectonically active regions around the Pacific Rim. We believe studies that include paleoseismic trenching and GPR are needed to refine the level of fault activity rate inferred from simple geomorphic analysis of active fault scarps and should be undertaken prior to or during early construction. Clearly, the correlation between faults activity rate and fault geomorphic expression will need to be assessed for each individual local region, as this correlation depends of the local rates of deposition (volcanism) and fault activity.

ACKNOWLEDGEMENTS

We thank Contact Energy Ltd. for the permission to present these data… This study was funded by Contact Energy Ltd. and GNS Core Funding. We appreciate the valuable review comments from Jon Carrey, Rob Langridge, Russ Van Dissen and Simon Nelis.

REFERENCES

Acocella, V., Spinks, K., Cole, J., and Nicol, A.: Oblique back arc rifting of Taupo Volcanic Zone, New Zealand. *Tectonics*, **22**, (2003), 1045.

Berryman, K.R., Villamor, P., Nairn, I.A., Van Dissen, R.J., Begg, J.G., and Lee, J.M.: Late Pleistocene surface rupture history of the Paeroa Fault, Taupo Rift, New Zealand. *New Zealand Journal of Geology and Geophysics*, **51**, (2008), 135-158.

Bibby, H.M., Caldwell, T.G., Davey, F.J., and Webb, T.H.: Geophysical evidence on the structure of the Taupo Volcanic Zone and its hydrothermal circulations, *Journal of Volcanology and Geothermal Research*, **68**, (1995), 29-58.

Bryan, C.J., Sherburn, S., Bibby, H.M., Bannister, S.C., and Hurst, A.W.: Shallow seismicity of the central Taupo Volcanic Zone, New Zealand: its distribution and nature, *New Zealand Journal of Geology and Geophysics*, **42**, (1999), 533-542.

Fellows, D. L.: Taupo Fault Belt: mapping. EDS Immediate report 89/1, EDS archive file number 381/3 (1989).

Gehrels, M.J., Lowe, D.J., Hazell, Z.J., and Newnham, R.M.: A continuous 55300-yr Holocene cryptotephrostratigraphic record from northern New Zealand and implications for tephrochronology and volcanic hazard assessment, *The Holocene*, **16**, (2006), 173-187.

Grindley, G.W.: The Geology, Structure, and Exploitation of the Wairakei Geothermal Field, Taupo, New Zealand, *New Zealand Geological Survey Bulletin*, **75**, (1965), 131 p.

Hajdas, I., Lowe, D.J., Newnham, R.M., and Bonani, G.: Timing of the late-glacial climate reversal in the Southern Hemisphere using high resolution radiocarbon chronology for Kaipo bog, New Zealand, *Quaternary Research*, **65**, (2006) 340–345.

Kerr, J., Nathan, S., Brunsdon, D., King, A., and Van Dissen, R.: Planning for development of land on or close to active faults, Institute of Geological and Nuclear Sciences Client Report 2002/124 (2003), (prepared for Ministry for the Environment, New Zealand). http://www.mfe.govt.nz/publications/rma/planning-development-active-faults-dec04/index.html.

Litchfield, N.J., Van Dissen, R.J., Sutherland, R., Barnes, P.M., Cox, S.C., Norris, R., Beavan, R.J., Langridge, R.M., Villamor, P.; Berryman, K.R., Stirling, M.W., Nicol, A., Nodder, S., Lamarche, G., Barrell, D.J.A., Pettinga, J.R., Little, T., Pondard, N., Mountjoy, J.J., and Clark, K.J.: A model of active faulting in New Zealand. *New Zealand Journal of Geology and Geophysics*, **57**, (2014), 32-56.

Manville, V.R. and Wilson, C.J.N.: The 26.5 ka Oruanui eruption, New Zealand: a review of the roles of volcanism and climate in the post-eruptive sedimentary response, *New Zealand Journal of Geology and Geophysics*, **47**, (2004), 525-547.

Massiot, C., McNamara, D.D., and Lewis, B.: Interpretive review of the acoustic borehole image logs acquired to date in the Wairakei-Tauhara Geothermal Field, GNS Science Report 2013/04. Institute of Geological and Nuclear Sciences Limited, Lower Hutt (2013).

McClymont, A.F., Villamor, P., and Green, A.G.: Fault displacement accumulation and slip rate variability within the Taupo Rift (New Zealand) based on trench and 3-D ground-penetrating radar data, *Tectonics*, **28**, (2009), TC4005.

McLean, K. and McNamara, D.: Fractures interpreted from acoustic formation imaging technology: correlation to permeability, Thirty-Sixth Workshop on Geothermal Reservoir Engineering Stanford University (2011).

McNamara, D., Massiot, C., and Lewis, B.: A structural review of Wairakei-Tauhara Geothermal Field. Lower Hutt: GNS Science. GNS Science report 2013/03, (2013).

Risk, G.F.: Electrical resistivity survey of the Wairakei Geothermal Field. Proceedings of the 6th New Zealand Geothermal Workshop, University of Auckland, New Zealand, (1984), 123–128.

Rosenberg, M.D., Bignall, G., and Rae, A.J.: The geological framework of the Wairakei-Tauhara Geothermal System, New Zealand, *Geothermics*, **38**, (2009), 72-84.

Rowland, J.V. and Sibson, R.H.: Extensional fault kinematics within the Taupo Volcanic Zone, New Zealand: soft-linked segmentation of a continental rift system, *New Zealand Journal of Geology and Geophysics*, **44**, (2001), 271-283.

Rowland, J.V. and Sibson, R.H.: Structural controls on hydrothermal flow in a segmented rift system, Taupo Volcanic Zone, New Zealand, *Geofluids*, **4**, (2004), 259-283.

Salvi, S., Cinti, F. R., Colini, L., D'Addezio, G., Doumaz, F., and Pettinelli, E.: Investigation of the active Celano–L'Aquila fault system, Abruzzi (central Apennines, Italy) with combined ground-penetrating radar and palaeoseismic trenching, *Geophysical Journal International*, **155**, (2003), 805-818.

Seebeck, H., Nicol, A., Stern, T.A., Bibby, H.M., and Stagpoole, V.: Fault controls on the geometry and location of the Okataina Caldera, Taupo Volcanic Zone, New Zealand, *Journal of Volcanology and Geothermal Research*, **190**, (2010), 136-151.

Sparks, R.J., Melhuish, W.H., McKee, J.W.A., Ogden, J., and Palmer, J.G.: ^{14}C calibration in the Southern Hemisphere and the date of the last Taupo eruption: evidence from tree-ring sequences, *Radiocarbon*, **37**, (1995), 155–163.

Spinks, K.D., Acocella, V., Cole, J.W., and Bassett, K.N.: Structural control of volcanism and caldera development in the transtensional Taupo Volcanic Zone, New Zealand, *Journal of Volcanology and Geothermal Research*, **144**, (2005), 7-22.

Vandergoes, M.J., Hogg, A.G., Lowe, D.J., Newnham, R.M., Denton, G.H., Southon, J., Barrell, D.J.A., Wilson, C.J.N., McGlone, M.S., Allan, A.S.R.;, Almond, P.C., Petchey, F., Dabell, K., Dieffenbacher-Krall, A.C., and Blaauw, M.: A revised age for the Kawakawa/Oruanui tephra, a key marker for the Last Glacial Maximum in New Zealand. *Quaternary Science Reviews*, **74**, (2013), 195-201.

Villamor, P., and Berryman, K.R.: A late Quaternary extension rate in the Taupo Volcanic Zone, New Zealand, derived from fault slip data, *New Zealand Journal of Geology and Geophysics*, **44**, (2001), 243-269.

Wilson, C.J.N.: Stratigraphy, chronology, styles, and dynamics of late Quaternary eruptions from Taupo volcano, New Zealand, *Philosophical Transactions of the Royal Society*, London, Serial A, **343**, (1993), 205-306.

Wilson, C.J.N., Houghton, B.F., McWilliams, M.O., Lanphere, M.A., Weaver, S.D., and Briggs, R.M.: Volcanic and structural evolution of Taupo Volcanic Zone, New Zealand: a review, *Journal of Volcanology and Geothermal Research*, **68**, (1995), 1-28.